

EIT IMAGE RECONSTRUCTION BASED ON GENETIC ALGORITHM VIA A TWO-STEP APPROACH

H.-C. Kim[†], D.-C. Moon[†], M.C. Kim^{††}, S. Kim^{†††}, and Y.J. Lee^{†††}

[†]*Dept. of Electrical Eng., Cheju National Univ., Cheju, 690-756, Korea,*

^{††}*Dept. of Chemical Eng. & Clean Tech., Cheju National Univ., Cheju, 690-756, Korea,*

^{†††}*Dept. of Nuclear and Energy Eng., Cheju National Univ., Cheju, 690-756, Korea,*

Abstract: In electrical impedance tomography (EIT), the internal resistivity distribution of the unknown object is computed with the boundary voltage data induced by different current patterns using various reconstruction algorithms. This paper presents a new image reconstruction algorithm based on genetic algorithm (GA) via two-step approach for the solution of the EIT inverse problem, in particular for the reconstruction of “static” images. The computer simulation for the 32 channels synthetic data shows that the spatial resolution of reconstructed images in the proposed scheme is improved compared to that of the modified Newton–Raphson algorithm at the expense of increased computational burden.

Keywords: Electrical impedance tomography, Genetic algorithms, Image reconstruction, Inverse problem.

1. INTRODUCTION

Electrical impedance tomography (EIT) plays an important role in monitoring tools for the process engineering such as biomedical, geological and chemical engineering, due to its relatively cheap electronic hardware requirements and nonintrusive measurement properties (Webster, 1990; Newell *et al.*, 1987; Cheney *et al.*, 1999). In EIT different current patterns are injected to the unknown object through electrodes and the corresponding voltages are measured on its boundary surface. The physical relationship between inner resistivity (or conductivity) and boundary surface voltage is governed by the nonlinear Laplace equation with appropriate boundary conditions so that it is impossible to obtain the closed-form solution for the resistivity distribution. Hence, the internal resistivity distribution of the unknown object is computed using the boundary voltage data based on various reconstruction algorithms.

Yorkey *et al.* (1987) developed a modified Newton-Raphson (mNR) algorithm for a static EIT image reconstruction and compared it with other existing algorithms such as backprojection, perturbation and double constraints methods. They concluded that the mNR reveals relatively good performance in terms of convergence rate and residual error compared to those of the other methods. However, in real situations, the mNR method is often failed to obtain satisfactory images from physical data due to large modeling error, poor signal to noise ratios (SNRs) and ill-conditioned (ill-posed) characteristics. That is, the ratio between the maximum and minimum eigenvalues of the information matrix (or Hessian matrix) is very large. In particular, the ill-

conditioning of the information matrix results in an inaccurate matrix inverse so that the resistivity update process is very sensitive to the modeling and measurement errors.

Genetic algorithms (GAs) have recently found extensive applications in solving global optimization searching problems (Goldberg, 1989). They are useful when the closed-form optimization technique cannot be applied. GAs are parallel, global search techniques that emulate natural genetic operators. Because a GA simultaneously evaluates many points in the parameter space, it is more likely to converge toward the global solution. It does not need to assume that the search space is differentiable or continuous, and can also iterate several times on each datum received. The GAs apply operators inspired by the mechanics of natural selection to a population of binary strings encoding the parameter space. At each generation, it explores different areas of the parameter space, and then directs the search to regions where there is a high probability of finding improved performance. By working with a population of solutions, the algorithms can in effect search for many local minima, and thereby increase the likelihood of finding the global minimum. Global optimization can be achieved via a number of genetic operators, e.g., reproduction, mutation, and crossover.

The major difficulties in impedance imaging are in the nonlinearity of the problem itself and the poor sensitivity of the boundary voltages to the resistivity of the flow domain deep inside. Several researchers suggested various element or mesh grouping methods where they force all meshes belonging to certain groups to have the same resistivity values

(Glidewell and Ng, 1995; Paulsen *et al.*, 1995).

In this paper, we will discuss the image reconstruction in EIT based on GA via a two-step approach. We have broken the procedure for obtaining the internal resistivity distribution into two parts. In the first step, each mesh is classified into three mesh groups: target, background, and temporary groups. The mNR algorithm can be used to determine the region of group. In the second step, the values of these resistivities are determined using genetic algorithm. The first GA searches for the optimal range of resistivities by generating and evolving a population of individuals whose chromosome consists of two real genes (\mathbf{r}_{back} and \mathbf{r}_{tar}) representing the values of the unknown background and target group's resistivity distribution. The second GA solves the EIT problem, searching for the resistivity values of meshes in temporary group. All meshes in temporary group can have different resistivity values. This two-step approach allows us to better constrain the inverse problem and subsequently achieve a higher spatial resolution.

2. MATHEMATICAL MODEL FOR EIT

2.1 The forward model

When electrical currents $I_l (l=1, \dots, L)$ is injected into the object $\Omega \in R^2$ through electrodes $e_l (l=1, \dots, L)$ attached on the boundary $\partial\Omega$ and the resistivity distribution $\mathbf{r}(x, y)$ is known over Ω , the corresponding induced electrical potential $u(x, y)$ can be determined uniquely from the nonlinear Laplace equation which can be derived from the Maxwell equation, Ohm's law, and the Neumann type boundary condition. The complete electrode model takes into account both the shunting effect of the electrode and the contact impedances between the electrodes and the object. The equations of complete electrode model are

$$\nabla \cdot (\mathbf{r}^{-1} \nabla u) = 0 \text{ in } \Omega \quad (1)$$

$$\int_{e_l} \mathbf{r}^{-1} \frac{\partial u}{\partial n} dS = I_l, \quad l = 1, \dots, L$$

$$u + z_l \mathbf{r}^{-1} \frac{\partial u}{\partial n} = U_l \text{ on } e_l, \quad l = 1, \dots, L \quad (2)$$

$$\mathbf{r}^{-1} \frac{\partial u}{\partial n} = 0 \text{ on } \partial\Omega \setminus \bigcup_{l=1}^L e_l$$

where z_l is effective contact impedance between the l th electrode and the object, U_l are the measured potentials and n is outward unit normal. In addition, we have the following two conditions for the injected currents and measured voltages by taking into account the conservation of electrical charge and

appropriate selection of ground electrode, respectively.

$$\sum_{l=1}^L I_l = 0, \quad (3)$$

$$\sum_{l=1}^L U_l = 0, \quad (4)$$

The computation of the potential $u(x, y)$ for the given resistivity distribution $\mathbf{r}(x, y)$ and boundary condition I_l is called the forward problem. The numerical solution for the forward problem can be obtained using the finite element method (FEM). In the FEM, the object area is discretized into small elements having a node at each corner. It is assumed that the resistivity distribution is constant within an element. The potential at each node is calculated by discretizing (1) into $Y\mathbf{u} = c$, where $Y \in R^{N \times N}$ is so-called stiffness matrix and N is the numbers of FEM nodes. Y and c are the functions of the resistivity distribution and the injected current patterns, respectively.

2.2 The Tikhonov regularization method

The inverse problem, also known as the image reconstruction, consists in reconstructing the resistivity distribution $\mathbf{r}(x, y)$ from potential differences measured on the boundary of the object. The methods used for solving the EIT problem search for an approximate solution, i.e., for a resistivity distribution minimizing some sort of residual involving the measured and calculated potential values. From a mathematical point of view, the EIT inverse problem consists in finding the coordinates of a point in a N -dimensional hyperspace, where N is the number of discrete elements whose union constitutes the tomographic section under consideration. In the past, several EIT image reconstruction algorithms for the current injection method have been developed by various authors. A review of these methods is given by Murai and Kagawa (1985). To reconstruct the resistivity distribution inside the object, we have to solve the nonlinear ill-posed inverse problem. The regularization techniques are needed to obtain stable solutions due to the ill-posedness.

Generalized Tikhonov regularized version of the EIT inverse problem can be written in the form

$$\Psi(\mathbf{r}) = \min_{\mathbf{r}} \{ \|V - U(\mathbf{r})\|^2 + \mathbf{a} \|R(\mathbf{r} - \mathbf{r}^*)\|^2 \} \quad (5)$$

where $\mathbf{r} \in R^N$ and \mathbf{r}^* are the resistivity distribution and *a priori* information of \mathbf{r} , respectively. $U(\mathbf{r}) \in R^{LK}$ is the vector of voltages obtained from the model with known \mathbf{r} , $V \in R^{LK}$ are the measured voltages and R and \mathbf{a} are the regularization matrix

and the regularization parameter, respectively. L , K , and M are the numbers of electrodes on the surface, injected current patterns, and finite elements in FEM respectively. There are many approaches in the literature (Cohen-Bacrie *et al.*, 1997; Vauhkonen *et al.*, 1996; Adler and Guardo, 1996; Grootveld *et al.*, 1998) to determine R and \mathbf{a} , but the usual choice is to fix $R = I_N$ and to adjust \mathbf{a} empirically.

Minimizing the objective function $\Psi(\mathbf{r})$ gives an equation for the update of the resistivity vector

$$\begin{aligned} \mathbf{r}^{k+1} &= \mathbf{r}^k + \Delta \mathbf{r}^{k+1} \\ \Delta \mathbf{r}^k &= (H_k + \mathbf{a}I)^{-1} \{J_k^T (V - U(\mathbf{r}^k)) - \mathbf{a}(\mathbf{r}^k - \mathbf{r}^*)\} \end{aligned} \quad (6)$$

where the partial derivative of Ψ with respect to \mathbf{r} has been approximately by a Taylor series expansion around \mathbf{r}^k . The Jacobian J_k is a matrix composed of the derivative of the vector of predicted potentials with respect to the unknown resistivities. The Jacobian is derived from the finite element formulation given by $J_k = \frac{\partial \Psi}{\partial \mathbf{r}} \Big|_{\mathbf{r}^k}$. The Hessian H_k

is the second derivative of the predicted potentials with respect to the resistivity. Since the objective function $\Psi(\mathbf{r})$ is multimodal (i.e., it presents several local minima), the inversion procedure does not always converge to the true solution. The reconstruction algorithms are likely to be trapped in a local minimum and sometimes the best solution of a static EIT problem is rather unsatisfactory.

3. IMAGE RECONSTRUCTION BASED ON GA VIA A TWO-STEP APPROACH

In some applications like visualization of two-component systems, we may assume that there are only two different representative resistivity values; one resistivity value for the background and the other for the target. In this paper, we will discuss the image reconstruction in EIT using two-step approach. We have broken the procedure for obtaining the internal resistivity distribution into two parts.

3.1 Step one – mNR method and mesh grouping

In the first step, we adopted a mNR method as a basic image reconstruction algorithm. After a few initial mNR iterations performed without any grouping, we classify each mesh into one of three mesh groups: BackGroup (or TargetGroup) is the mesh group with the resistivity value of the background (or target). TempGroup is the group of meshes neither in BackGroup nor in TargetGroup. All meshes in BackGroup and in TargetGroup are forced to have the same but unknown resistivity value (\mathbf{r}_{back} and \mathbf{r}_{tar}), respectively. However, all

meshes in TempGroup can have different resistivity values ($\mathbf{r}_{temp,i}$, $i = 1, \dots, n-2$).

Let s_i ($i = 1, \dots, n$) be the resistivity distribution after this rearrangement. Then, the typical shape of s_i becomes the curve shown in Fig. 1 during the reconstruction process. In Fig. 1, it is natural to assume that meshes in regions I and III belong to BackGroup and TargetGroup, respectively. All meshes in region II can be classified into TempGroup.

However, since we cannot always expect to get such a well-distinguished resistivity distribution curve as shown in Fig. 1, it is useful to divide the regions and determine a typical resistivity value of each region. Let \bar{r}_i ($i = 1, \dots, 3$) be the representative resistivity value in each region and k_i ($i = 1, 2$) be the boundary location between regions. Then, we can formulate the following optimization problem to determine \bar{r}_i and k_i :

$$J(x) = \min_x \left\{ \sum_{i=1}^3 \sum_{j=k_{i-1}}^{k_i} (s_j - \bar{r}_i)^2 \right\} \quad (7)$$

where $x = (\bar{r}_1, \bar{r}_2, \bar{r}_3, k_1, k_2)$, $k_0 = 1$, and $k_2 = n$.

We solve the problem in (7) using the GA and the solution provides one way of dividing regions (Cho *et al.*, 2001).

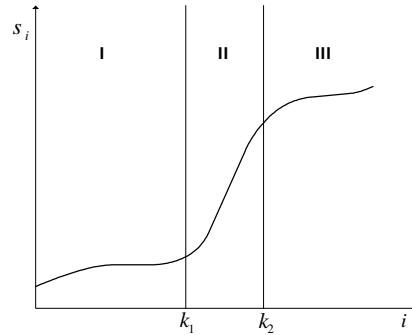


Fig. 1. Typical distribution of the sorted resistivity values during image reconstruction.

3.2 Step two – Image reconstruction based on the genetic algorithm

In the second step, a set (population) of EIT images is generated for the simplest implementation of GA in EIT. Each individual consists in a n -tuple of resistivity values (n is the number of elements discretizing the section under measurement), i.e., the EIT chromosome is a sequence of n resistivities. After mesh grouping, in this paper, we will determine the values of these resistivities using two GAs. The first GA searches for the optimal range of resistivities by generating and evolving a population of individuals whose chromosome consists of two

real genes (\mathbf{r}_{back} and \mathbf{r}_{tar}), representing the BackGroup and TargetGroup values of the unknown resistivity distribution. All meshes in background and in target group are forced to have the same but unknown resistivity value (\mathbf{r}_{back} and \mathbf{r}_{tar}), respectively. Furthermore, we will use \mathbf{r}_{back} (or \mathbf{r}_{tar}) as the minimum (or maximum) values of the unknown resistivity distribution. The second GA solves the EIT problem, searching for the resistivity distribution ($\mathbf{r}_{temp,i}, i = 1, \dots, n-2$) minimizing the reconstruction error. The computed resistivities is constrained between the minimum and maximum values obtained in the first GA.

A fitness value is computed for each individual. In the present case, the fitness function is the reciprocal of the reconstruction error, a function of the relative difference between the computed and measured potentials on the object boundary

$$f_c = \frac{L(L-1)}{2} \left[\sum_{i=1}^{L(L-1)/2} \left| \frac{V_i(\mathbf{r}) - U_i}{U_i} \right| \right]^{-1} \quad (8)$$

where L is the number of electrodes on the surface. The next stage is to rank the individuals on the fitness value, giving the fitter ones more chance to contribute to the successive generation. New individuals are then created by crossover (combination of couples of resistivity sequences) and mutation (low-probability random change of some resistivity value in the genome).

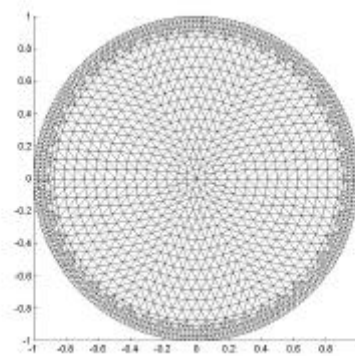
After this stage, the chosen termination criterion is applied, i.e., we see if convergence has been reached (the residue is below a given value) or if the maximum number of generations has been exceeded. If convergence fails, the whole selection+crossover+mutation procedure is applied to the current population, otherwise the fittest individual is assumed as the solution of the EIT problem. The termination condition adopted here is based on evaluating the progress made by the algorithm in a predefined number of generations and terminating the search if the fitness of the best chromosome is above a threshold value.

4. COMPUTER SIMULATION

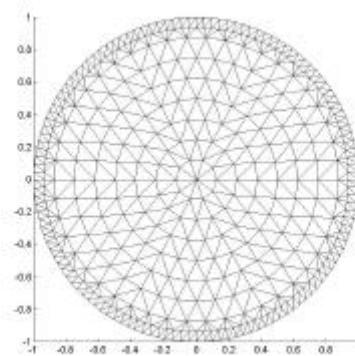
The proposed algorithm has been tested by comparing its results for numerical simulations with those obtained by the modified Newton-Raphson (mNR) method. For the current injection the trigonometric current patterns were used. For the forward calculations, the domain Ω was a unit disc and the mesh of 3104 triangular elements ($M=3104$) with 1681 nodes ($N=1681$) and 32 channels ($L=32$) was used as shown in Fig. 2(a). A different mesh system with 776 elements ($M=776$) and 453 nodes ($N=453$) was adopted for the inverse calculations as

shown in Fig. 2(b). In this paper, under the assumption that the resistivity varies only in the radial direction within a cylindrical coordinate system, the results of the two inverse problem methods can be easily compared. The resistivity profile given to the finite element inverse solver varies from the center to the boundary of object and is divided into 9 radial elements ($\mathbf{r}_1, \dots, \mathbf{r}_9$) in Fig. 2(b).

The resolution of the method is determined by a number of variables including resistivity contrast and distribution, position within the domain, and even current patterns. The ability to positively distinguish between two similar resistivity distributions also depends upon the precision of the voltage measurements. These factors necessitate caution when designing an experiment and interpreting results. Therefore, to verify the appropriateness of EIT for this application, a computational experiment was conducted.



(a)



(b)

Fig. 2. Finite element mesh used in the calculation. (The resistivities of the elements within an annular ring are identical.) (a) mesh for forward solver, (b) mesh for inverse solver.

Synthetic boundary potentials were computed for idealized resistivity distributions using the finite element method described earlier. The boundary potentials were then used for inversion and the results were compared to the original resistivity

profiles. The resistivity profile appearing in Fig. 3 has a step change at $r/R=0.43$. The inverted profile using mNR method matches the original profile very well near the boundary of the object at $r/R=1$ and the jump in resistivity was located successfully. However, the inverse method using mNR searches for a resistivity profile which is smooth, which explains the deviation near the center at $r/R=0$ and the boundary of target and background at $r/R=0.43$.

We started the mNR iteration without any mesh grouping with a homogeneous initial guess. In Table 1, we see that the mNR algorithm may roughly estimate the given true resistivities. Since the mNR have a large error at the boundary of target and background in Fig. 3, we can not obtain reconstructed images of high spatial resolution. This kind of poor convergence is a very typical problem in the NR-type algorithms.

However, we can significantly improve the mNR's poor convergence by adopting the proposed GA via a two-step approach as follows.

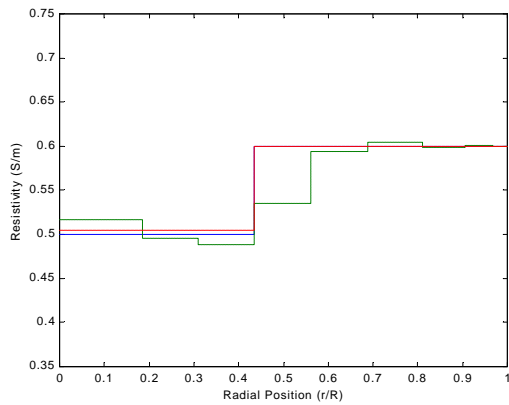


Fig. 3. True resistivities (solid line) and computed resistivities using mNR (dashed line) and GA (dotted line).

Table 1. True resistivities and computed resistivities using mNR and GA

	\mathbf{r}_1	\mathbf{r}_2	\mathbf{r}_3	\mathbf{r}_4	\mathbf{r}_5	\mathbf{r}_6	\mathbf{r}_7	\mathbf{r}_8	\mathbf{r}_9
Real	0.5	0.5	0.5	0.6	0.6	0.6	0.6	0.6	0.6
mNR	.516	.495	.489	.535	.594	.604	.599	.601	.600
GA	.505	.505	.505	.600	.600	.600	.600	.600	.600

In the first step, we adopted a mNR method as a basic image reconstruction algorithm. After a few initial mNR iterations performed without any grouping, we classify each mesh into one of three mesh groups. After the mesh grouping in (7), we could obtain the following result that 2 meshes ($\mathbf{r}_2, \mathbf{r}_3$) and 5 meshes ($\mathbf{r}_5, \mathbf{r}_6, \mathbf{r}_7, \mathbf{r}_8, \mathbf{r}_9$) among 9 are grouped to TargetGroup (\mathbf{r}_{tar}) and BackGroup

(\mathbf{r}_{back}), respectively. The remainders of meshes ($\mathbf{r}_1, \mathbf{r}_4$) are grouped to TempGroup. Hence, the number of unknowns is reduced to 4.

In the second step, after mesh grouping, we will determine the values of these resistivities using two GAs. The first GA searches for the optimal range of resistivities by generating and evolving a population of individuals whose chromosome consists of two real genes (\mathbf{r}_{back} and \mathbf{r}_{tar}), representing the BackGroup and TargetGroup values of the unknown resistivity distribution. Furthermore, we will use \mathbf{r}_{back} (or \mathbf{r}_{tar}) as the minimum (or maximum) values of the unknown resistivity distribution. $\bar{\mathbf{r}}_1$ and $\bar{\mathbf{r}}_3$ in (7) are used the initial value of \mathbf{r}_{tar} and \mathbf{r}_{back} in BackGroup and TargetGroup, respectively. Table 2 shows the computed resistivities as a function of the population size at generation 200. The reconstructed errors at a given generation generally decrease when the population size is increased. Hence, even if error does not depend linearly on the population size due to the stochastic nature of GA's, 40 or 60-individual GA reconstruction gives a higher spatial resolution than a mNR method.

Table 2. True and computed resistivities using GA vs population size at generation 200

Pop. size	\mathbf{r}_{back}		\mathbf{r}_{tar}	
	True	Computed	True	Computed
20	0.5	0.4898	0.6	0.6000
40	0.5	0.5051	0.6	0.6001
60	0.5	0.4998	0.6	0.6039

The second GA solves the EIT problem, searching for the resistivities of remainders ($\mathbf{r}_1, \mathbf{r}_4$) minimizing the reconstruction error. The computed resistivities in this second GA is constrained between the minimum and maximum values obtained in the first GA. In Fig. 3, the inverted profile using GA matches the original profile very well near the wall at $r/R=1.0$ as well as the center at $r/R=0.0$. Furthermore, the GA reconstruction is practically perfect for the jump of resistivity at $r/R=0.43$.

4. CONCLUSION

In this paper, an EIT image reconstruction method based on GA via two-step approach was presented to improve the spatial resolution. A technique based on two binary-coded GA's with the knowledge of mNR was developed for the solution of the EIT inverse problem. One GA calculates the resistivity values of target group and background group, and the other GA is used to search for the resistivities of remainders. Although GA is expensive in terms of computing time and resources, which is a weakness

of the method that renders it presently unsuitable for real-time tomographic applications, the exploitation of *a priori* knowledge will produce very good reconstructions. Further extensions include an EIT image reconstruction to multi-resistivity value problems.

Tomography, Adam Hilger.
Yorkey, T.J., J.G. Webster and W.J. Tompkins (1987). Comparing reconstruction algorithms for electrical impedance tomography, *IEEE Trans. on Biomedical Engineering*, **34**, 843-852.

ACKNOWLEDGEMENT

This work was supported by the Nuclear Academic Research Program by the Ministry of Science and Technology (MOST).

REFERENCES

- Adler, A. and R. Guardo (1996). Electrical impedance tomography: regularized imaging and contrast detection, *IEEE Trans. on Medical Imaging*, **15**, 170-179.
- Cheney, M, D. Isaacson and J.C. Newell (1999). Electrical impedance tomography, *SIAM Review*, **41**, 85-101.
- Cho, K.H., S. Kim and Y.J. Lee (2001). Impedance imaging of two-phase flow field with mesh grouping method. *Nuclear Engineering and Design*, **204**, 57-67.
- Cohen-Bacrie, C., Y. Goussard and R. Guardo (1997). Regularized reconstruction in electrical impedance tomography using a variance uniformization constraint, *IEEE Trans. on Medical Imaging*, **16**, 170-179.
- Goldberg, D.E. (1989). *Genetic Algorithms in Search, Optimization and Machine Learning*. Reading, MA: Addison Wesley.
- Glidewell, M. and K.T. Ng (1995). Anatomically constrained electrical impedance tomography for anisotropic bodies via a two-step approach, *IEEE Trans. on Medical Imaging*, **14**, 498-503.
- Grootveld, C.J., A. Segal and B. Scarlett (1998). Regularized modified Newton-Raphson technique applied to electrical impedance tomography, *International Journal of Imaging System Technology*, **9**, 60-65.
- Murai, T. and Y. Kagawa (1985). Electrical impedance computed tomography based on a finite element model, *IEEE Trans. on Biomedical Engineering*, **32**, 177-184.
- Newell, J.C., D.G. Gisser and D. Isaacson (1987). An electric current tomograph, *IEEE Trans. on Biomedical Engineering*, **35**, 828-833.
- Paulsen, K.D., P.M. Meaney, M.J. Moskowitz and J.M. Sullivan (1995). A dual mesh scheme for finite element based reconstruction algorithm, *IEEE Trans. on Medical Imaging*, **14**, 504-514.
- Vauhkonen, M., D. Vadasz, P.A. Karjalainen, and J. P. Kaipio (1996). Subspace regularization method for electrical impedance tomography, *1st International Conference on Bioelectromagnetism*, Tampere, Finland, 9-13.
- Webster, J.G. (1990). *Electrical Impedance*